Acta Crystallographica Section D
Biological Crystallography
ISSN 0907-4449

The structure of substrate-free microbial ribonuclease binase and of its complexes with 3′GMP and sulfate ions

K. M. Polyakov,[a] A. A. Lebedev,[a,b]* A. L. Okorokov,[c] K. I. Panov,[d] A. A. Schulga,[e] A. G. Pavlovsky,[f] M. Ya. Karpeisky[a]† and G. G. Dodson[g]

[a]Institute of Crystallography, RAS, 107333 Moscow, Russia, [b]School of Crystallography, Birkbeck College, London WC1E 7HX, England, [c]Department of Biology, University of York, York YO10 5DD, England, [d]Division of Gene Regulation and Expression, Wellcome Trust Biocentre, University of Dundee, Dundee DD1 5HE, Scotland, [e]Shemyakin and Ovchinnikov Institute of Bioorganic Chemistry, RAS, 107333 Moscow, Russia, [f]Discovery Technologies, Pfizer Global Research and Development, Ann Arbor, Michigan 48105, USA, and [g]Department of Chemistry, University of York, York YO10 5DD, England

† Deceased 19 July 2000.

Correspondence e-mail: a.lebedev@cryst.bbk.ac.uk

Received 29 October 2001
Accepted 18 February 2002

PDB References: binase, 1gou, r1gousf; binase complex with sulfate ions, 1gov, r1govsf; binase complex with 3′GMP, 1goy, r1goysf.

The structures of *Bacillus intermedius* ribonuclease (binase), an extracellular 109-residue enzyme, and its complexes with 3′GMP and sulfate ions were solved at 1.65 and 2.0 Å, respectively. The structures were refined using *REFMAC*. The crystal of free binase belongs to the space group *C*2, whereas the crystals of complexes belong to the space group $P2_12_12_1$. In both crystal lattices the asymmetric unit contains two molecules which form an identical dimer. The structure of the dimer is such that only one of its subunits can bind the nucleotide in the 3′GMP–binase complex, where the guanyl base is located in the recognition loop of the enzyme. In both binase complex structures the phosphate group of 3′GMP or one of the sulfate ions make an electrostatic interaction with the binase molecule at the catalytic site. A second phosphate-binding site was found in the structures of the complexes at the cleft formed by the loop 34–39, the main chain of Arg82 and the side chain of Trp34. Comparison of the complex and unliganded enzyme crystal structures shows that there are some small but distinct differences in the specificity loop (56–62) and in the loops 34–39 and 99–104 associated with the binding of the nucleotide and sulfate ions.

1. Introduction

Extracellular ribonuclease from *Bacillus intermedius* (RNase Bi; binase; EC 3.1.27.3) is a single-chain polypeptide consisting of 109 amino-acid residues with a molecular mass of 12.3 kDa. Binase belongs to a family of highly processive microbial ribonucleases (Hartley, 1980; Hill *et al.*, 1983). The binase molecule contains no cysteines or cystines and no cofactors or associated metal ions. It cleaves single-stranded ribonucleic acids (RNA) after purines, producing mono- and oligoribonucleotides with the phosphate left at the 3′-hydroxyl group of the terminal ribose. This is a two-step reaction. The first step (transesterification) gives rise to RNA-chain cleavage and formation of 2′:3′-cyclophosphate; the second step results in hydrolysis of the cyclophosphate by an activated water molecule (Okorokov *et al.*, 1997).

The structures of several guanyl-specific ribonucleases and their complexes with guanosine 3′-monophosphate (3′GMP), the product of the reaction, have been determined to high resolution (Baudet & Janin, 1991; Sevcik *et al.*, 1991, 1993; Martinez-Oyanedel *et al.*, 1991; Zegers *et al.*, 1994; Buckle & Fersht, 1994; Martin *et al.*, 1999). The guanine-specificity of microbial RNases was shown to originate from oriented interactions between a nucleotide base and recognition site of protein (Sevcik *et al.*, 1990). The fungal (T1-like) ribonucleases recognize the guanyl base with high efficiency in RNA substrates of any length (Takahashi & Moor, 1982). The

bacillus ribonucleases such as binase or barnase (RNase Ba), which exhibit 85% amino-acid sequence homology (Hill *et al.*, 1983), only have high guanyl specificity towards cyclophosphates or short RNA fragments (less than four nucleotides).

The hydrolysis rate of oligonucleotides ($Xp_0Gp_1Xp_2Xp_3$ or shorter) by the RNase barnase strongly depends on the presence of the P2 phosphate group (Day *et al.*, 1992). This phosphate group was observed to be bound by the protein molecule at the side chain of Arg82 in the crystal structure of the barnase complex with d($Cp_0Gp_1Ap_2C$) (Buckle & Fersht, 1994). The presence of the second phosphate-binding site appears to be a reason for the significant decrease of guanyl specificity in bacterial RNases, *e.g.* barnase or binase, compared with T1-like RNases.

In this paper, we report the crystal structure of unliganded (free) binase solved and refined at 1.65 Å resolution using *BLANC* (Vagin *et al.*, 1998) and *REFMAC* (Murshudov *et al.*, 1997). With this structure, we analyse the influence of substrate and ion binding on the enzyme's local mobility and conformation by comparing it with structures of 3′GMP and sulfate-ion complexes. The structures of these two complexes were previously solved at 2.0 Å resolution (Pavlovsky *et al.*, 1983, 1989; Pavlovsky & Karpeisky, 1989) and have been refined further using *REFMAC*.

2. Methods

2.1. Crystallization and data collection

The crystals of wild-type binase complexes with 3′GMP and sulfate were obtained (Pavlovsky *et al.*, 1989) by co-crystallization using the vapour-diffusion technique. The crystals of sulfate complex were grown in 35 µl sitting drops containing 12–13 mg ml^{-1} protein, 12% PEG 12 000, 25 m*M* phosphate buffer pH 7.0 and 3% saturated ammonium sulfate. The reservoir contained 23–24% PEG 12 000 in 50 m*M* glycine buffer at pH 7.0. The crystallization conditions for the 3′GMP complex were almost the same as those for the sulfate complex except that the saturated solution of the mononucleotide was added to the drops at a four- to fivefold excess with respect to the protein. The crystals of both complexes belong to the space group $P2_12_12_1$. In both cases the unit-cell parameters are a = 111.4, b = 69.6, c = 33.5 Å and the unit cell contains two protein molecules per asymmetric unit. Single-crystal diffraction data for the binase complexes were collected to 2.0 Å resolution at room temperature on a Syntex $P2_1$ diffractometer.

The recombinant binase was expressed and purified as described previously (Shulga *et al.*, 1994; Okorokov *et al.*, 1994; Panov, 1994). Two forms of recombinant binase were obtained, one correctly processed and the other with seven extra N-terminal residues (FTPVTKA) left from the *phoA* signal secretory peptide. Crystals of the recombinant binase with seven extra residues were obtained by vapour diffusion at room temperature from a 5 mg ml^{-1} solution of the enzyme buffered with 50 m*M* glycine and 2.5% sodium citrate pH 9. The reservoir contained 20% PEG 10 000 in the same buffer. The crystals belong to space group *C*2, with unit-cell parameters a = 115.0, b = 33.3, c = 78.7 Å, γ = 119.1°, and contain two protein molecules in the asymmetric unit. Diffraction data to 1.65 Å resolution were collected from an unliganded binase crystal at room temperature using the synchrotron-radiation source at EMBL-Hamburg. Crystals of the correctly processed enzyme suitable for X-ray study could not be grown.

Table 1
Summary of X-ray data, refinement and model statistics.

Values in parentheses are for the outermost resolution shell.

	RNase Bi, wild type, 3′GMP complex	RNase Bi, wild type, SO_4^{2-} complex	RNase Bi, recombinant, unliganded
PDB code	1goy	1gov	1gou
Crystallographic data			
Space group	$P2_12_12_1$	$P2_12_12_1$	$C2$
Unit-cell parameters			
a (Å)	111.4	111.4	115.0
b (Å)	69.6	69.6	33.3
c (Å)	33.5	33.5	78.7
β (°)	—	—	119.1
Resolution range (Å)	24.9–2.00 (2.05–2.00)	55.7–2.00 (2.05–2.00)	15.0–1.65 (1.69–1.65)
No. of observations	15152	18301	95418
No. of unique reflections	15152	18301	30591
Completeness (%)	82.9 (34.2)	99.8 (97.9)	96.0 (94.1)
R_{merge}† (%)	—	—	3.9 (13.0)
$\langle I/\sigma(I)\rangle$	5.1 (1.8)	6.3 (1.9)	16.6 (7.3)
Resolution shell with $\langle I/\sigma(I)\rangle \simeq 3$ (Å)	2.74–2.60	2.38–2.30	—
Refined model			
R factor (%)	18.4	19.1	14.0
R_{free} (%)	—	—	17.6
R.m.s. deviations from standard values			
Bond lengths (Å)	0.019	0.017	0.018
Bond angles (°)	2.2	2.0	2.1
No. of non-H atoms in			
Protein molecules	1731	1733	1773
3′GMP molecule	24	—	—
SO_4^{2-} ions	15	20	—
Water molecules	183	182	255
Average B factors (Å^2)			
Protein main chains	23.6	22.5	22.1
Protein side chains	25.2	24.4	24.5
3′GMP	33.4	—	—
SO_4^{2-} ions	28.1	35.7	—
Water molecules	37.0	36.0	38.6
Percentage of residues‡ in Ramachandran plot regions			
Most favoured	85.1	87.2	86.3
Additional allowed	13.3	12.2	13.2
Generously allowed	1.6	0.6	0.5

† Not defined for non-redundant data sets. ‡ Excluding Pro, Gly and terminal residues.

2.2. Structure determination and refinement

The structures of the complexes of binase with 3′GMP and sulfate were initially solved and refined by Pavlovsky *et al.* (1983, 1989). Refinement using *REFMAC* (Murshudov *et al.*, 1997) revealed a second phosphate-binding site and allowed us to correct the solvent structure and some of the side-chain and main-chain atom positions. Here, we describe these revised crystal structures.

The structure of unliganded binase was solved by molecular replacement using *BLANC* (Vagin *et al.*, 1998), with the starting model formed by two protein molecules constituting the asymmetric unit in the 3′GMP complex structure. The structure was refined using *REFMAC*.

Data and refinement statistics for the three structures are given in Table 1. Electron-density maps covering the active site of molecule *A* are shown for the 3′GMP complex and unliganded binase structures in Figs. 1(*a*) and 1(*b*), respectively.

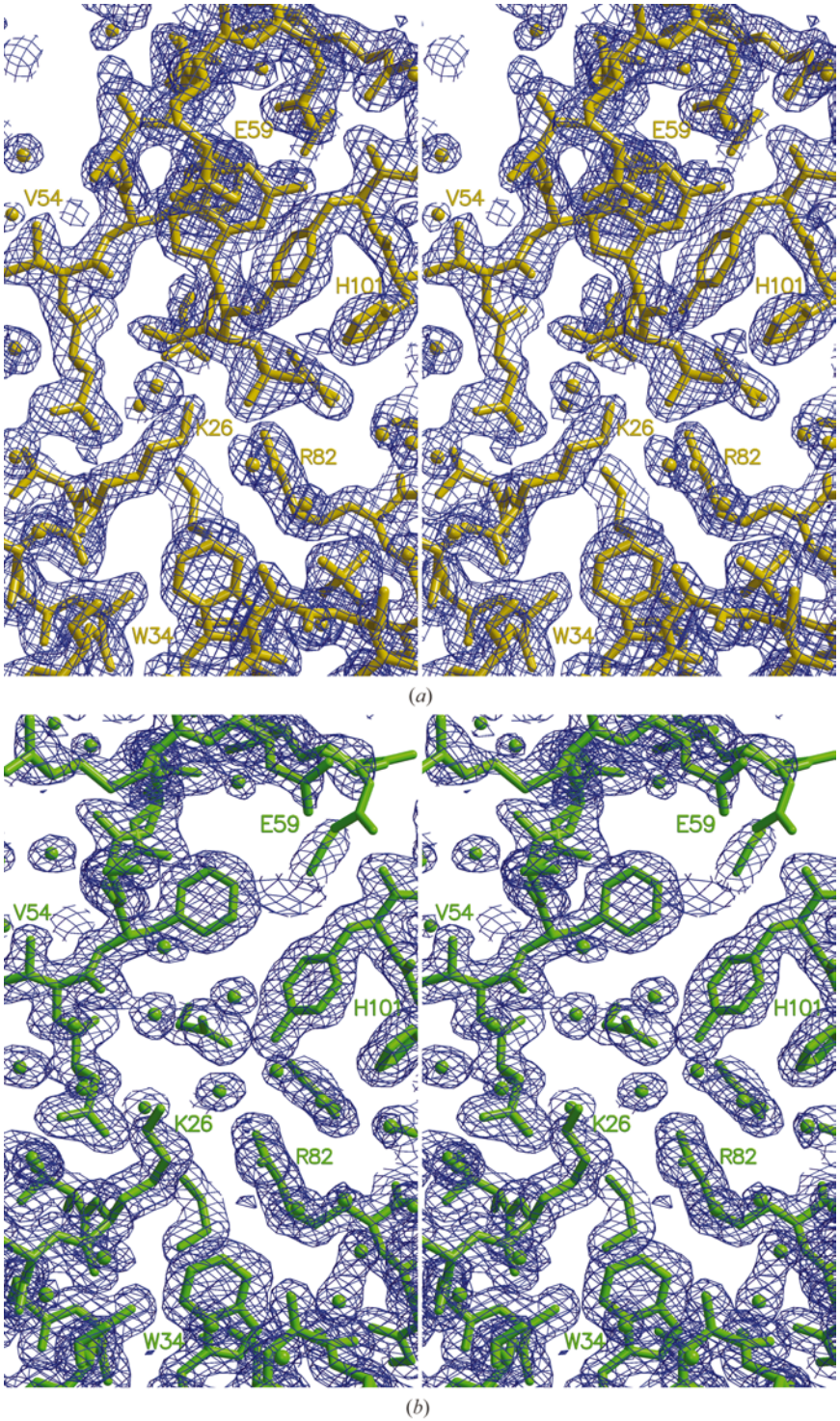

Figure 1
A stereoview of the electron-density map ($2F_o - F_c$) covering the binase active and P2 sites (*a*) in the 3′GMP complex structure and (*b*) in the unliganded binase structure. The contouring level is at 1σ. This figure was generated using *MOLSCRIPT* (Kraulis, 1991), *BOBSCRIPT* (Esnouf, 1997) and *Raster3D* (Merritt & Bacon, 1997).

3. Results and discussion

3.1. Overall folding of the binase molecule and crystal packing

Binase is an $\alpha\beta$ protein as displayed in Fig. 2. It contains a central β-sheet of five antiparallel strands (residues 49–55, 70–75, 85–90, 95–98 and 106–109) and three α-helices (residues 5–16, 26–32 and 41–44). The binase overall fold is generally identical to that of barnase, the RNase from *B. amyloliquefaciens* (Mauguen *et al.*, 1982). The main-chain fold and especially the central β-sheet are identical in all six binase molecules in the three crystal structures under consideration.

In the binase crystals, the molecules are arranged as layers made up of closely packed dimers. The contacts within the layers are similar in the two crystal forms (see Fig. 3); however, those between the layers are very different. Analysis of the interatomic contacts suggests that the interactions between molecules *A* and *B* (highlighted in Fig. 3) are the strongest between neighbouring pairs of molecules. These two molecules have essentially identical contacts in the two different space groups and form the same dimer. The molecules in the dimer are packed without rotational symmetry, as can be seen in Fig. 3. The dimer structure is stabilized by eight hydrogen bonds, including a possible salt bridge between the side chains of Glu43 and Arg58, and by hydrophobic interaction between the side chain of Phe81 (molecule *A*) and the side chains of Tyr102 and His101 (molecule *B*). These last two residues form part of the active site, which is consequently blocked. The side chain of Phe81 of molecule *A* partly occupies the guanine base binding site of molecule *B*. Accordingly, the nucleotide is observed only in molecule *A* of the binase–3′GMP complex. The above fact and the fact that the crystal of the complex was obtained by co-crystallization allow us to assume that a similar binase dimer may occur in solution at high protein concentration. The presence of a binase dimer in solution has been also demonstrated by Panov (1995). The sequence change from

Glu43 to Asp44, the equivalent residue in barnase, may be the reason why no similar dimer was observed in barnase crystals.

3.2. 3′GMP and phosphate-binding sites

Consistent with the crystal packing discussed above, electron density corresponding to 3′GMP was found only in molecule *A* of the dimer in the binase–3′GMP complex. The electron density of the nucleotide is well defined (Fig. 1*a*) and its atoms have the same thermal parameters as surrounding buried protein atoms.

The interactions of the guanine base with its protein environment in the binase–3′GMP complex have been discussed previously (Pavlovsky & Karpeisky, 1989; Sevcik *et al.*, 1990, 1991). They are essentially the same as in the barnase–3′GMP (Guillet *et al.*, 1993) and barnase–d(CGAC) (Buckle & Fersht, 1994) complexes. The guanyl base is accommodated in the hydrophobic cleft formed by the side chains of Phe55 and Tyr102 and the aliphatic moiety of Arg58. In addition, it makes a set of hydrogen bonds with the side and main chains of residues from the recognition loop (residues 56–62) of the binase molecule.

In the 3′GMP complex the torsion glycoside angle χ (O4′—C1′—N9—O4) is 133°, *i.e.* it belongs to the *anti*-conformation region. The ribose ring has the 2′-*endo* conformation. The nucleotide conformation in the binase complex with 3′GMP differs from the productive *syn* conformation of the substrate seen in the active site of the enzyme (Guillet *et al.*, 1993). Consequently, the ribose O2′ atom is directed away from the catalytic Glu72. A similar conformation of the guanosine nucleotide was detected in the structure of the barnase–d(CGAC) complex (Buckle & Fersht, 1994).

The ions involved in the crystal structures were modelled and refined as sulfate ions. This is an arbitrary notation as long as both sulfate and phosphate ions were present in the mother liquor; these ions cannot be distinguished in the structures on the basis of available X-ray data. The sulfate ion bound by the binase molecule at the P1 site of the sulfate-complex structure forms hydrogen bonds with the side chains of Lys27, Glu72, Arg82, Tyr102, His101 and Arg86. The 3′-phosphate group at the P1 site forms contacts similar to those seen in the sulfate complex (Fig. 4). The only significant difference is that the *anti* conformation (non-productive) of the nucleotide causes the side chain of Glu72 to be rotated away from the 3′-phosphate group, preventing their hydrogen-bond contact in the 3′GMP complex.

The putative second phosphate-binding site P2 was found in the structures of binase complexes with 3′GMP and sulfate in the cleft formed by the loop 34–39, the main chain of Arg82 and the side chain of Trp34. The binding of an ion here is illustrated in Fig. 4. The electron-density peak corresponding to this ion has tetrahedral character (Fig. 1*a*). This site appears to bind the 3′-phosphate group of the nucleotide following the guanyl in the polynucleotide substrate. The position of the sulfate ion at the P2 site is 2.6 Å distant from the position of the adenosine 3′-phosphate group in the structure of the d(CGAC)–barnase complex (Buckle & Fersht, 1994) and the guanosine 3′-phosphate group in the structure of the d(GC)–barnase complex (Baudet & Janin, 1991). The phosphate group in the latter two structures has moved out the cleft towards the side chain of the arginine. This difference may be caused by a non-productive conformation of the guanyl nucleotide in the active site of the d(CGAC)–barnase complex.

3.3. Comparison of the binase structures

Comparison of all six binase molecules from the three separate crystal structures shows their high similarity. The overall r.m.s. difference in C^{α}-atom positions, based on the superposition of the C^{α} atoms in the β-sheets, ranges from 0.17 to 0.33 Å. The maximal difference is observed between the *A* molecules in the 3′GMP complex structure and in the unliganded binase structure. All significant differences relate to

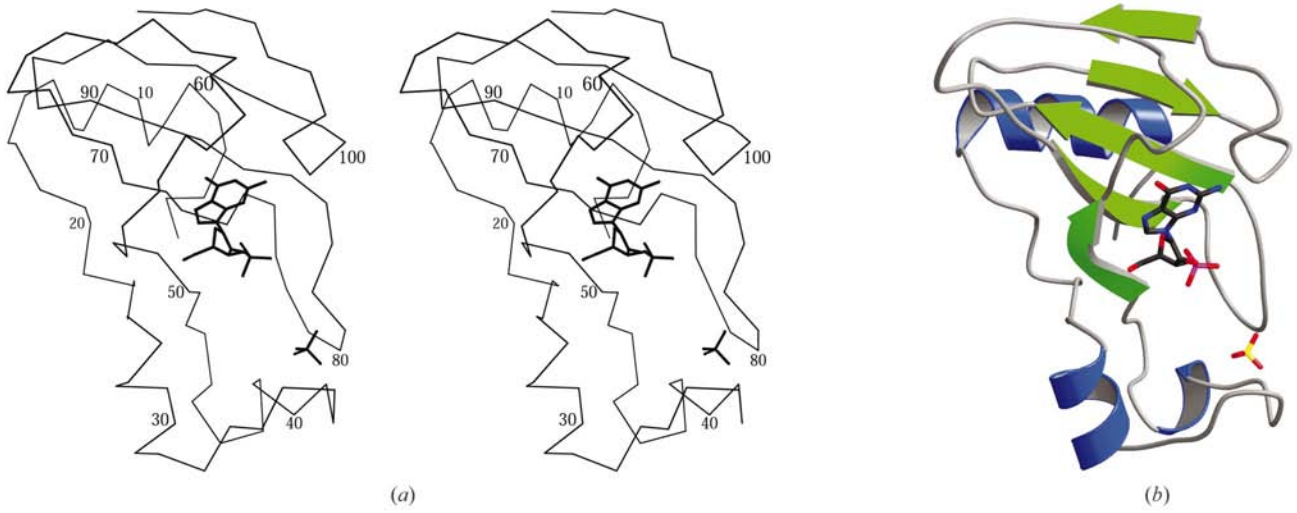

Figure 2
(*a*) A stereoview of the C^{α} trace with every tenth C^{α} numbered and (*b*) the ribbon diagram of binase (*MOLSCRIPT*, *Raster3D*). The 3′GMP molecule and sulfate ion are shown as bond models.

the loop regions (residues 34–39, 56–62 and 99–104); the recognition loop (residues 56–62) and loop 99–104 move toward each other in the complex structures (Fig. 4).

The conformation of the loop formed by residues 34–39 in the free binase structure is similar to that seen in all the barnase structures, free and complexed, so far studied and is not significantly influenced by contacts with symmetry-related molecules. The sulfate binding at the P2 site in the 3′GMP and sulfate complexes causes substantial changes in the loop compared with the free binase structure (Figs. 1 and 4). The carbonyl group of Ala36 is rotated by about 180° from its position in the free binase structure. The conformation of Ser37 ($\varphi = 110°$ and $\psi = -20°$) in the complexes falls near the boundary of the generally allowed region in the Ramachandran plot, but this conformation of the loop allows one of the sulfate O atoms to form hydrogen bonds with two main-chain N atoms (residues 37 and 39). This interaction helps to stabilize the unfavourable conformation of the loop 34–39.

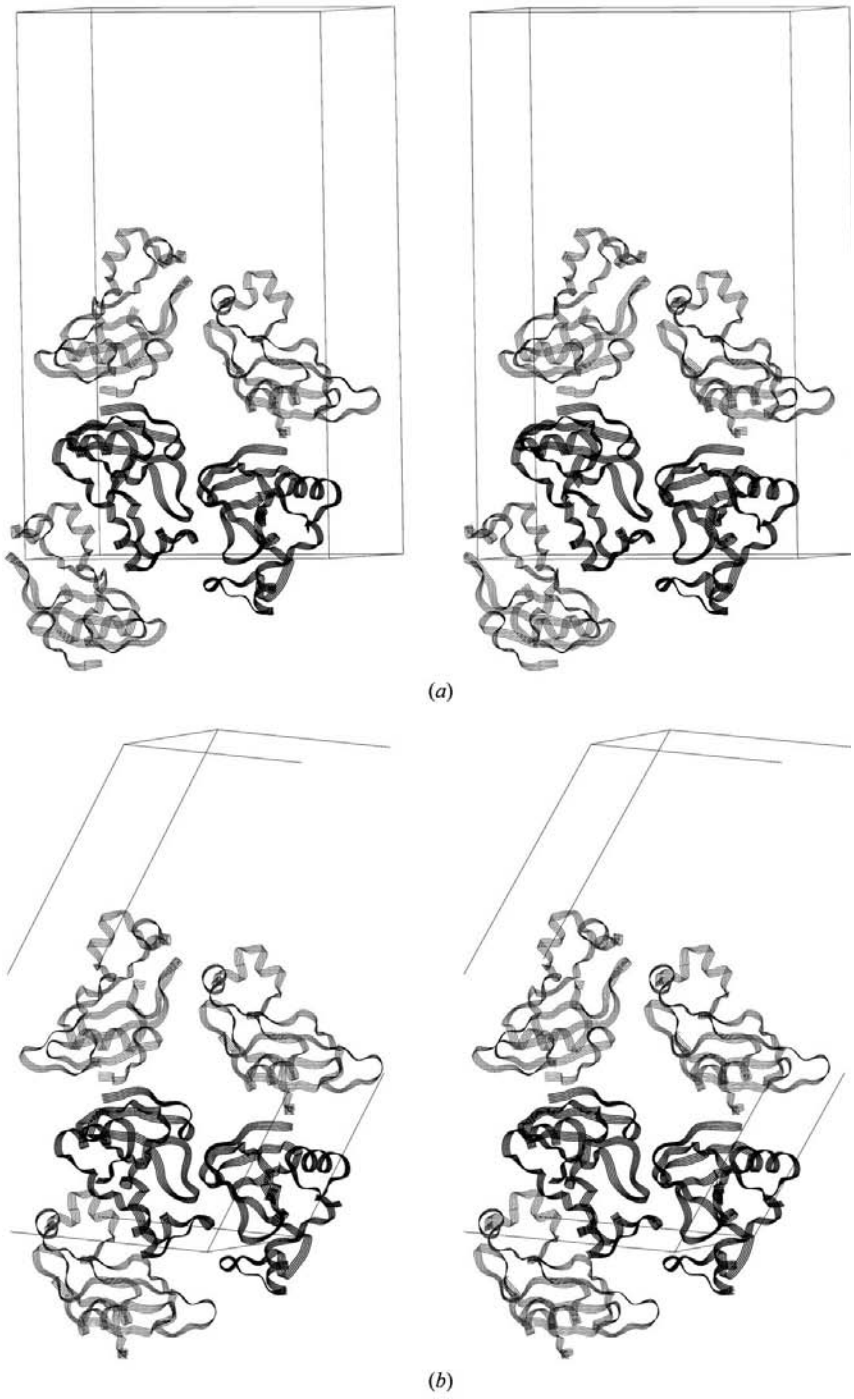

Figure 3
A stereoview of similar molecular layers in the (*a*) binase–3′GMP complex and (*b*) the unliganded binase structures (*QUANTA*). The two binase molecules forming a dimer are highlighted.

Comparison of atomic temperature factors shows that the recognition loop (residues 56–62) is more mobile in the unliganded binase structure, where the main chain of residues 56–57 has two conformations and the side chains of Arg58 and Glu59 have poorly defined electron density (Fig. 1*b*). In contrast, the recognition loop in the structure of the 3′GMP–binase complex is stabilized by interaction with the guanine base, yielding significantly lower temperature factors for the loop atoms. The conformation of the Arg58 side chain is determined by its interaction with the base; its aliphatic C atoms lie against the aromatic guanosine ring, making favourable non-polar contacts. The side chain of Glu59 has well defined electron density (Fig. 1*a*). Thus, there evidently exists one well determined conformation of loop 56–62 in both the binase and barnase complex structures in which the guanyl base occupies the base-binding site G0 and a phosphate group or ion is present at the P1 site. In the structures with no ligands at both G0 and P1 sites the loop is more removed from the active site and has a variable conformation influenced by interatomic contacts. The variation in C^{α} position is maximal (up to 2 Å) for residue 59.

The loop 99–104 is better defined than the recognition loop but appears to have two distinct states depending on the presence of an ion or phosphate group at the P1 site of the protein. The movement of this loop toward the active site is a response to the interaction of an O atom of the ligand with the side chains of Tyr102 and His101. In both states the conformation of the loop is not significantly influenced by the crystal environment and identical conformations occur in the barnase crystal structures.

There are 17 water molecules with similar positions in all six molecules in the three structures (Fig. 5). Ten of these waters have equivalents in the unliganded barnase struc-

ture (Martin *et al.*, 1999). These water molecules are a constitutive part of the binase molecule, stabilizing the secondary structure (grey circles in Fig. 5) and the protein conformation at the active site (black circles in Fig. 5).

Three water molecules in the free-enzyme structure are displaced in the complex by the 3′GMP ligand, which replaces their hydrogen-bond interactions with the protein. One water is located at the 3′-phosphate position, another is close to the position of the ribose C1 atom and the third is located between the N7 and C8 atoms of the base (Fig. 4).

Overall, comparison of the crystal structures of binase in its unliganded and nucleotide/ion-bound forms enables us to observe subtle changes in enzyme conformation associated with substrate binding.

This work was funded by the Royal Society, grant RC/JP.April99, and by the Russian Foundation for Fundamental Research, grants Nos. 99-02-16191 and 00-15-96633. We thank A. N. Popov for the help with the data collection at EMBL-Hamburg outstation. We also thank BBSRC for providing the computing facilities, grant No. 87/SB09829.

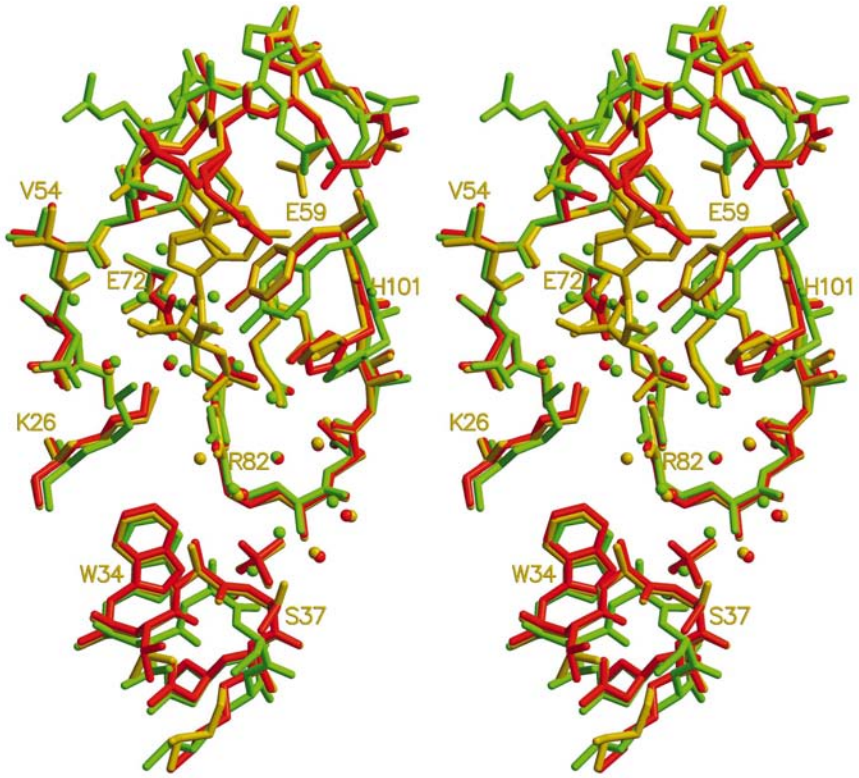

Figure 4
A stereoview of the superimposed active and P2 sites of molecule *A* in binase complexes with 3′GMP (yellow) and sulfate ions (red) and in unliganded binase (green), generated with *MOLSCRIPT* and *Raster3D*.

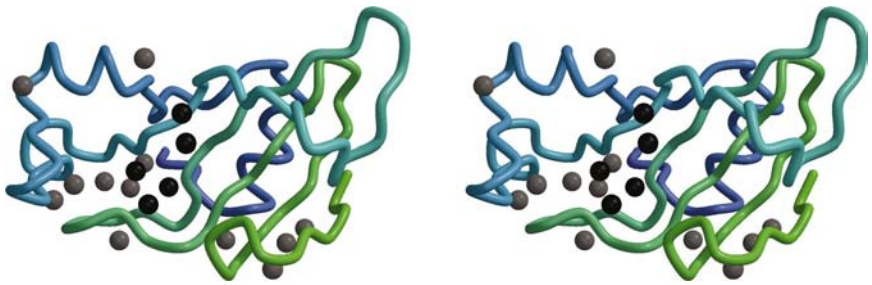

Figure 5
The ribbon stereo diagram of binase and conserved water molecules (*BOBSCRIPT*, *Raster3D*). The black circles correspond to water molecules located in the catalytic site.

References

Baudet, S. & Janin, J. (1991). *J. Mol. Biol.* **219**, 123–132.
Buckle, A. M. & Fersht, A. R. (1994). *Biochemistry*, **33**, 1644–1653.
Day, A. G., Parsonage, D., Ebel, S., Brown, T. & Fersht, A. R. (1992). *Biochemistry*, **31**, 6390–6395.
Esnouf, R. M. (1997). *J. Mol. Graph.* **15**, 132–134.
Guillet, V., Lapthorn, A. & Mauguen, Y. (1993). *FEBS Lett.* **330**, 137–140.
Hartley, R. W. (1980). *J. Mol. Evol.* **15**, 355–358.
Hill, C., Dodson, G., Heinemann, U., Saenger, W., Mitsui, Y., Nakamura, K., Borisov, S., Tischenko, G., Polyakov, K. & Pavlovsky, A. (1983). *Trends Biochem. Sci.* **8**, 364–369.
Kraulis, P. J. (1991). *J. Appl. Cryst.* **24**, 946–950.
Martin, C., Richard, V., Salem, M., Hartley, R. & Mauguen, Y. (1999). *Acta Cryst.* D**55**, 386–398.
Martinez-Oyanedel, J., Choe, H. W., Heinemann, U. & Saenger, W. (1991). *J. Mol. Biol.* **222**, 335–352.
Mauguen, Y., Hartley, R. W., Dodson, E. J., Dodson, G. G., Bricogne, G., Chothia, C. & Jack, A. (1982). *Nature (London)*, **297**, 154–162.
Merritt, E. A. & Bacon, D. J. (1997). *Methods Enzymol.* **277**, 505–524.
Murshudov, G. N., Vagin, A. A. & Dodson, E. J. (1997). *Acta Cryst.* D**53**, 240–255.
Okorokov, A. L., Hartley, R. W. & Panov, K. I. (1994). *Protein Expr. Purif.* **5**, 547–552.
Okorokov, A. L., Panov, K. I., Offen, W. A., Mukhortov, V. G., Antson, A. A., Karpeisky, M. Y., Wilkinson, A. J. & Dodson, G. G. (1997). *Protein Eng.* **10**, 273–278.
Panov, K. I. (1994). *J. Chromatogr. A*, **670**, 229–233.
Panov, K. I. (1995). PhD thesis. Engelhard Institute of Molecular Biology, Moscow, Russia.
Pavlovsky, A. G. & Karpeisky, M. Y. (1989). *Structure and Chemistry of Ribonucleases. Proceedings of the First International Meeting*, y & K. M. Polyakov, pp. 303–314. Moscow: USSR Academy of Sciences.
Pavlovsky, A. G., Sanishvili, R. G., Borisova, S. N., Strokopytov, B. V., Vagin, A. A., Chepurnova, N. K. & Vainshtein, B. K. (1989). *Kristalografiya*, **34**, 137–141. In Russian.
Pavlovsky, A. G., Vagin, A. A., Vainstein, B. K., Chepurnova, N. K. & Karpeisky, M. Y. (1983). *FEBS Lett.* **162**, 167–170.
Sevcik, J., Dodson, E. J. & Dodson, G. G. (1991). *Acta Cryst.* B**47**, 240–253.
Sevcik, J., Sansishvili, R. G., Pavlovsky, A. G. & Polyakov, K. M. (1990). *Trends Biochem. Sci.* **15**, 158–162.
Sevcik, J., Zegers, I., Wyns, L., Dauter, Z. & Wilson, K. S. (1993). *Eur J. Biochem.* **216**, 301–315.

Shulga, A. A., Okorokov, A. L., Panov, K. I., Kurbanov, F. T., Chernov, B. K., Kirpichnikov, M. P. & Scryabin, K. G. (1994). *Moleculyarnaya Biologiya*, **28**, 453–463. In Russian.
Takahashi, K. & Moor, S. (1982). *The Enzymes*, Vol. 15, 3rd ed., edited by P. D. Boyer, pp. 435–463. New York: Academic Press.
Vagin, A. A., Murshudov, G. N. & Strokopytov, B. V. (1998). *J. Appl. Cryst.* **31**, 98–102.
Zegers, I., Haikal, A. F., Palmer, R. & Wyns, L. (1994). *J. Biol. Chem.* **269**, 127–133.